JOURNAL OF MATERIALS SCIENCE 27 (1992) 1651–1658

Transient cavity growth in ceramics under compression

K. S. CHAN, R. A. PAGE
Southwest Research Institute, 6220 Culebra Road, PO Drawer 28510 San Antonio, Texas 78228-0510, USA

The transient cavity growth behaviour of liquid phase-sintered ceramics subject to compressive loads is examined. Three possible sources of transient behaviour are suggested, and their ranges of applicability evaluated. By considering the values of the characteristic time for individual transient modes, it has been determined that transient cavity growth in ceramics probably originates from transient grain-boundary sliding. Assuming that the creep-induced cavities nucleate and grow on grain boundaries that are parallel to the loading axis, a transient cavity growth model is developed on the basis that the local stress which drives cavity growth is induced by transient sliding of adjacent grain boundaries. Results of the proposed model are compared with small-angle neutron scattering measurements of a hot-pressed silicon carbide and a liquid phase-sintered alumina, both of which contain a continuous, amorphous grain-boundary phase. The different cavity growth behaviours observed in these ceramics are discussed in conjunction with transient grain-boundary sliding.

1. Introduction

The kinetics of cavity growth in a number of ceramics have been studied by Page and co-workers [1–5] using the small-angle neutron scattering (SANS) technique. These efforts have shown that the volume, V, of an individual cavity at time, t, after nucleation can be expressed as [1–6]

$$V = \alpha t^{\beta} \quad (1)$$

where α and β are empirical constants. Values of β ranging from 0.0 to 0.62 have been observed. The SANS measurements thus indicate that cavity growth in ceramics subject to compression is generally a transient process. The transient cavity growth behaviour of an AD99 alumina ceramic crept at 1150 °C and 220 MPa is illustrated in Fig. 1. In several other cases, the creep cavities were found to exhibit no apparent growth, as shown in Fig. 2 for the AD99 and Lucalox alumina. This condition of zero cavity growth, corresponding to $\beta = 0$, has been interpreted to mean that the cavities experienced a growth transient of short duration that was beyond the detection limit of the experimental measurements.

The growth of cavities in ceramics under compressive loads was analysed by Chan *et al.* [7] for steady-state conditions. Treating the constrained growth of cavities in a ceramic containing a continuous glassy grain-boundary phase, Chan *et al.* envisaged cavities growing on boundaries in response to a local boundary normal stress that arose due to grain boundary sliding, as depicted in Fig. 3a. The growth behaviour depicted by the dashed curve in Fig. 1 was calculated using this model by assuming steady-state grain-boundary sliding. From Fig. 1, it is obvious that the model of Chan *et al.* [7], or any other steady-state cavity-growth model, would not be adequate for describing the transient or zero growth behaviour observed in AD99 alumina and in other similar ceramics.

The transient growth of cavities by diffusion along grain boundaries subjected to a remotely applied tensile load was previously studied by Raj [8] using a Fourier-series approach. Sliding of grain boundaries under transient conditions was also analysed. The results of Raj suggest that more than one form of transient is possible. The objective of this paper is to identify the relevant mechanism(s) responsible for the growth transient observed in ceramics. The relevant mechanism will then be used to extend the model of Chan *et al.* [7] to treat transient cavity growth in ceramics either with (Fig. 3a) or without (Fig. 3b) a continuous grain boundary amorphous phase. Although there is evidence which shows that the creep cavities are oblate spheroids [7], only the growth of spheroidal cavities is to be considered. The proposed model will be compared with experimental results obtained by the SANS technique, and used to identify material parameters which influence conditions for transient growth, no growth, and possible shrinkage of creep cavities in ceramics subject to compressive loads.

2. Origins of cavity growth transients

Before presenting the transient cavity growth model, it is instructive to examine the possible origins of the cavity growth transient. It is worthwhile to note that transient cavity growth was observed in ceramics both with and without an amorphous grain boundary

0022–2461

phase. Transient cavity growth is therefore not associated with transient creep resulting from percolation or viscous flow of the grain boundary phase from boundaries under compression to those under tension. Instead, the cavity growth transient is thought to arise from stochastic grain-boundary sliding, as is continuous cavity nucleation [9]. This rationale is supported by a recent study [10] on creep of copper containing a liquid bismuth intergranular phase, which indicated that the creep strain associated with liquid-phase enhanced creep resulted primarily from grain-boundary sliding, and only a small creep strain ($\approx 0.1\%$) resulted from percolation of the liquid phase. Furthermore, a theoretical analysis [11] has revealed that the transient tensile creep strain resulting from percolation is $\approx 0.12f$, where f is the volume fraction of the liquid phase. For most liquid-phase sintered ceramics, the volume fraction of the grain-boundary amorphous phase is approximately 1%, yielding a transient creep strain of the order of 0.1%. Based on these results, transient creep in ceramics containing a continuous grain-boundary amorphous phase can be expected to

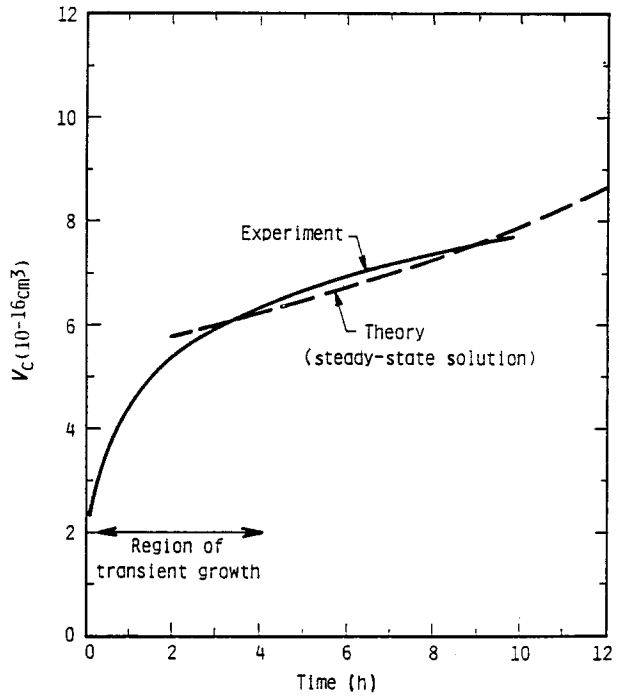

Figure 1 Comparison of SANS measurements of cavity volume, V_c, with the steady-state calculation of Chan *et al.* [7]. $R_0 = 51.5$ nm; $h_0 = 150$ nm; $l = 100$ nm; $\dot{\varepsilon} = 1 \times 10^{-7} s^{-1}$.

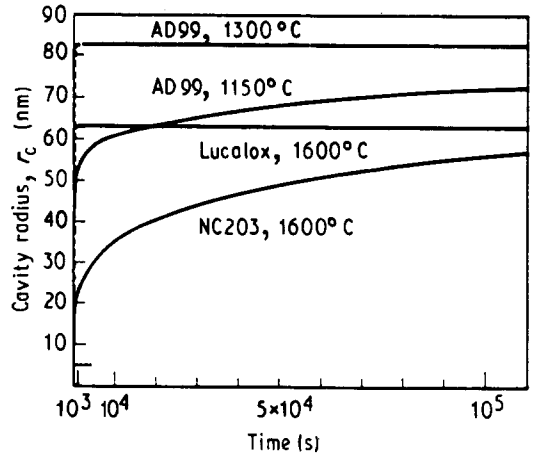

Figure 2 Increase in individual cavity radius with time [6].

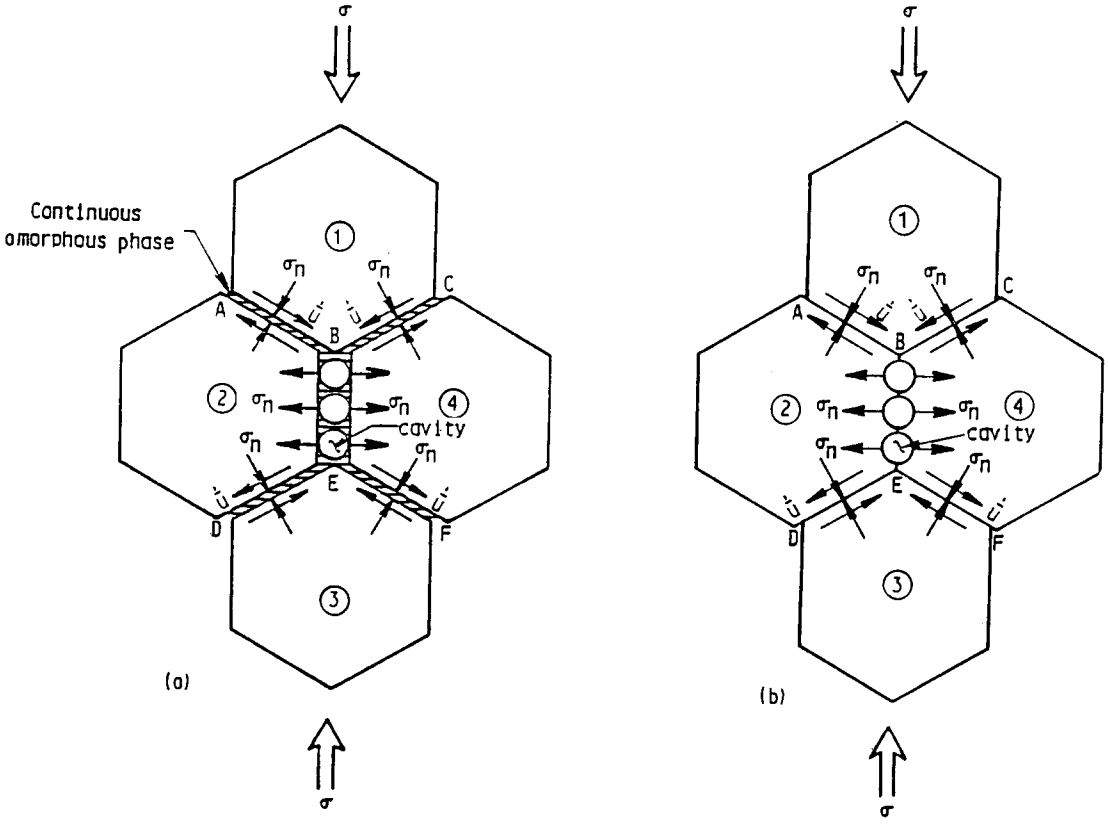

Figure 3 The cavity growth model of Chan *et al.* [7] for ceramics in compression: (a) with a continuous grain-boundary amorphous phase; (b) without a grain-boundary amorphous phase

arise primarily from transient grain-boundary sliding and not from percolation.

Grain-boundary sliding generally requires accommodation by contiguous grains [12]. The accommodated flow processes can be grain-boundary diffusion in ceramics without a grain-boundary vitreous phase [8, 12], but a solution precipitation process [13, 14] in one with a continuous amorphous phase along grain boundaries. The rate-controlling step in the latter might be either the kinetics of solution and precipitation, or the transport of atoms from regions of high stress to regions of low stress [13, 14]. For diffusional creep by grain-boundary diffusion [12] and transport limited solution–precipitation creep [14], the creep rates can both be described [12, 15] by

$$\dot{\varepsilon}_C \propto \frac{\Omega D_b h \sigma}{kTd^3} \tag{2}$$

where Ω is the atomic volume, D_b is the diffusion coefficient, h is the grain boundary height, σ is the local normal stress, k is Boltzmann's constant, T is temperature, and d is the grain size.

After nucleation of cavities by stochastic grain-boundary sliding, transient growth of these cavities can arise from three possible origins: (1) the transient grain boundary traction involved in the cavity nucleation process; (2) the transient normal traction that exists along the grain boundary between the nucleation event and the attainment of stress redistribution between the cavities; and (3) the transient tractions associated with grain boundary sliding transients. For all three cases, the characteristic time, t_c, is given by [8, 16]

$$t_c = \frac{32(1-\nu^2)L^3 kT}{\pi^3 E D_b h \Omega} \tag{3}$$

where ν is Poisson's ratio, E is Young's modulus, and L is the characteristic diffusion length.

It is noted that Equation 3 was obtained for transient grain-boundary sliding and cavity growth involving diffusion along clean grain boundaries [8]. Because of similar rate-controlling mechanisms and creep rate equations between diffusional creep by grain-boundary diffusion and the transport-limited solution precipitation creep, Equation 3 is considered to be applicable to creep of ceramics containing a continuous liquid phase along the grain boundary when the relationship [12]

$$\eta = \frac{1}{132}\frac{d^3 kT}{hD_b\Omega} \tag{4}$$

is invoked for relating the viscosity of the liquid phase to the grain-boundary diffusivity.

TABLE I Characteristic times for stress relaxation at various microstructural features in AD99 alumina crept at 1150 °C.

Microstructural feature	Size(m)	Characteristic time (s)
Ledge height	1×10^{-8}	3×10^{-7}
Cavity spacing	1×10^{-7}	3×10^{-4}
Grain size	20×10^{-6}	3×10^{3}(0.75 h)
	37×10^{-6}	2×10^{4}(4.7 h)

The calculations are based on material constants from Frost and Ashby [17]: $\Omega = 4.2\times10^{-29}\,m^3$, $hD_b = 2.7\times10^{-21}\,m^3\,s^{-1}$, $E = 3.2\times10^5$ MPa and $k = 1.38\times10^{-23}\,J\,K^{-1}$.

The characteristic diffusion length for the stress transient associated with cavity nucleation at grain-boundary ledges is the ledge height, which is of the order of 10 nm. For conditions representative of the SANS measurements, this diffusion length leads to a characteristic time of approximately 10^{-7} s, as presented in Table I. Obviously this short duration cannot possibly account for the cavity growth transient of 5 h shown in Fig. 1. Thus the stress transient associated with the nucleation event can be ruled out as a possible cause of the observed growth transients. The characteristic diffusion length for the stress transient associated with stress redistribution between a row of cavities is the cavity spacing, which is in the order of 100 nm for the AD99 alumina [7]. The corresponding characteristic time is 10^{-4} s (see Table I), which is also too small to account for the experimentally observed transients. The characteristic diffusion length for grain-boundary sliding is of the order of the grain size, however, which is 20–37 μm for the AD99 alumina. This relatively large diffusion length leads to a characteristic time ranging from 0.75 to 4.7 h, which is of the same order as the duration of the experimental transient. Based on these results, it is apparent that the experimentally observed growth transients are likely to originate from grain-boundary sliding transients. Furthermore, the transients associated with cavity nucleation and the relaxation of normal stress on the ligament between two cavities are of such short duration that they can generally be ignored.

3. The transient cavity growth model

The growth of creep cavities in ceramics subject to compression has been analysed previously by Chan *et al.* [7]. Treating constrained cavity growth in ceramics containing a continuous glassy grain-boundary phase, Chan *et al.* envisaged cavities growing on boundaries oriented parallel to the applied normal compressive stress in response to the sliding of contiguous grain boundaries, as depicted in Fig. 3. Their analysis of growth under conditions of steady-state grain-boundary sliding shows that the cavity growth rate, $\dot{R}$, for spheroidal cavities is given by [7]

$$\dot{R} = \frac{h^2 G(\xi)}{8\pi\eta R}[\sigma_n - 2\gamma_s K(1 - 0.9\xi^2)] \tag{5}$$

with

$$\xi = R/l$$

and

$$G(\xi) = \frac{2\sqrt{3} - 0.667\pi\xi^2}{0.96\xi^2 - \ln\xi - 0.23\xi^4 - 0.72} \tag{6}$$

where R is the cavity radius, η is the viscosity of the glassy phase, l is the cavity spacing, γ_s is the surface energy, and K is a constant related to the ratio of the grain boundary, surface, and interfacial energies. The average normal stress, σ_n, on the vertical boundary is

related to the steady-state creep rate, $\dot{\varepsilon}_{ss}$, due to grain-boundary sliding [7]

$$\sigma_n = \frac{33\eta\dot{\varepsilon}_{ss}}{2\pi} \quad (7)$$

which is substituted into Equation 5 to obtain

$$\dot{R} = \frac{h^2 G(\xi)}{8\pi\eta R}\left[\frac{33\eta\dot{\varepsilon}_{ss}}{2\pi} - 2\gamma_s K(1 - 0.9\xi^2)\right] \quad (8)$$

relating the growth rate of cavities located along the vertical boundary BE to the strain rate associated with the sliding of contiguous grain boundaries (AB, BC, DE, and EF). If sliding along these grain boundaries is transient, the growth of cavities on boundary BE would generally not be described by Equation 8 because it was derived for steady-state conditions only. On the other hand, the large difference between the characteristic time for the stress relaxation at the cavity ligament and the characteristic time for grain-boundary sliding suggests that a steady-state condition would prevail at the cavity ligament long before it could be reached at adjacent grain boundaries. Thus a quasi steady-state stress distribution would be expected to exist between the cavities even during transient sliding. Under these circumstances, the transient cavity growth rate may be obtained by replacing the $\dot{\varepsilon}_{ss}$ term in Equation 8 by the creep rate, $\dot{\varepsilon}_{tr}$, that accompanies transient grain-boundary sliding.

The creep rate for grain boundaries undergoing transient sliding has been analysed by Raj using a Fourier series method [8]. The grain-boundary shapes considered in the analysis included triangular, hexagonal, and a combination of these. The results of this work, presented in Fig. 4, indicate that the transient and the steady-state creep rates are related by

$$\dot{\varepsilon}_{tr}/\dot{\varepsilon}_{ss} = (t/t_c)^m \quad (9)$$

with the value of m lying between -0.5 and -0.6. Although Equation 9 has been developed for transient sliding of clean grain boundaries, which are accommodated by diffusion, it is anticipated that the form of the expression is valid for sliding of grain boundaries containing a continuous amorphous phase, providing

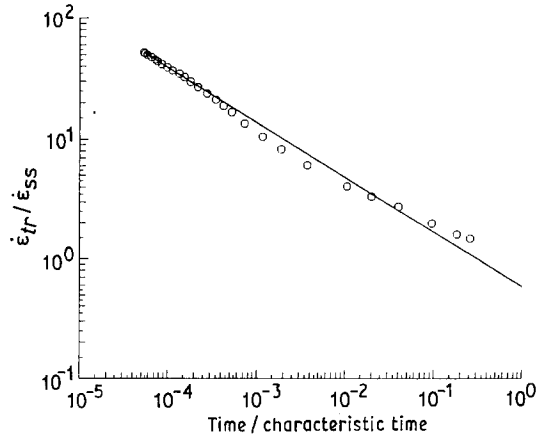

Figure 4 Power-law fit of Raj's calculation [8] of transient creep rate, $\dot{\varepsilon}_{tr}$, due to grain-boundary sliding as a function of time normalized by the characteristic time to reach the steady-state creep rate, $\dot{\varepsilon}_{ss}$.

that the appropriate value of t_c is used. Despite the fact that a theoretical value of -0.5 to -0.6 has been obtained, it is recognized that the experimental value for m might vary with individual ceramics or alloys. Based on these assumptions, substituting Equation 9 into the transient sliding equivalent of Equation 8 leads to

$$\dot{R} = \frac{h^2 G(\xi)}{8\pi\eta R}\left[\frac{33\eta\dot{\varepsilon}_{ss}(t/t_c)^m}{2\pi} - 2\gamma_s K(1 - 0.9\xi^2)\right] \quad (10)$$

which can be simplified to give

$$\dot{R} = \frac{33RG(\xi)}{4\pi^2}\left[\dot{\varepsilon}_{ss}(t/t_c)^m - \frac{4\pi}{33}\left(\frac{\gamma_s}{\eta l}\right)(1/\xi - 0.9\xi)\right] \quad (11)$$

when $h = 2R$ and $K = 1/R$ for spheroidal cavities are invoked, leading to

$$\dot{\xi} = \frac{33\xi G(\xi)}{4\pi^2}\left[\dot{\varepsilon}_{ss}(t/t_c)^m - \frac{4\pi}{33}\left(\frac{\gamma_s}{\eta l}\right)(1/\xi - 0.9\xi)\right] \quad (12)$$

and finally

$$\xi = \int \frac{33\xi G(\xi)}{4\pi^2}\left[\dot{\varepsilon}_{ss} t_c \tau^m - \frac{4\pi}{33}\left(\frac{\gamma_s t_c}{\eta l}\right) \times (1/\xi - 0.9\xi)\right] d\tau \quad (13)$$

with $d\tau = dt/t_c$ as the governing equations for cavity growth under transient grain-boundary sliding.

4. Effects of transient grain-boundary sliding on cavity growth

The first term contained in the bracket of Equation 13 is the transient creep rate which drives cavity growth, while the second term corresponds to the cavity sintering rate, $\dot{s}$, given by

$$\dot{s} = \frac{4\pi}{33}\left(\frac{\gamma_s}{\eta l}\right)(1/\xi - 0.9\xi) \quad (14)$$

From Equations 12 and 14, it is evident that the cavity growth rate, $\dot{\xi}$, depends on the values of ξ, $\dot{s}$, and $\dot{\varepsilon}_{tr}$. Since both $\dot{\xi}$ and $\dot{s}$ depend on ξ, interactions of these quantities are expected.

The growth behaviour of creep cavities subject to the influence of transient grain-boundary sliding has been examined by numerical integration of Equation 13 using the simple Euler method. In these calculations, the value of m was set at -0.5, while the ratio $\gamma_s t_c/\eta l$ was set at 0.194. The initial value of ξ, ξ_0 was 0.01, corresponding to an initial cavity radius of 1 nm for a cavity spacing of 100 nm. The transient cavity-growth model is assumed to apply when $t > 0.01 t_c$, which is considerably longer than the time required for the steady-state condition to occur at the ligament between cavities, but is much too short for the steady-state condition to occur at adjacent sliding grain boundaries. Thus, the initial condition is $\xi_0 = 0.01$ at $t = t_0 = 0.01 t_c$. This value of t_0 corresponds to an initial stress concentration factor of 3.16, which is a

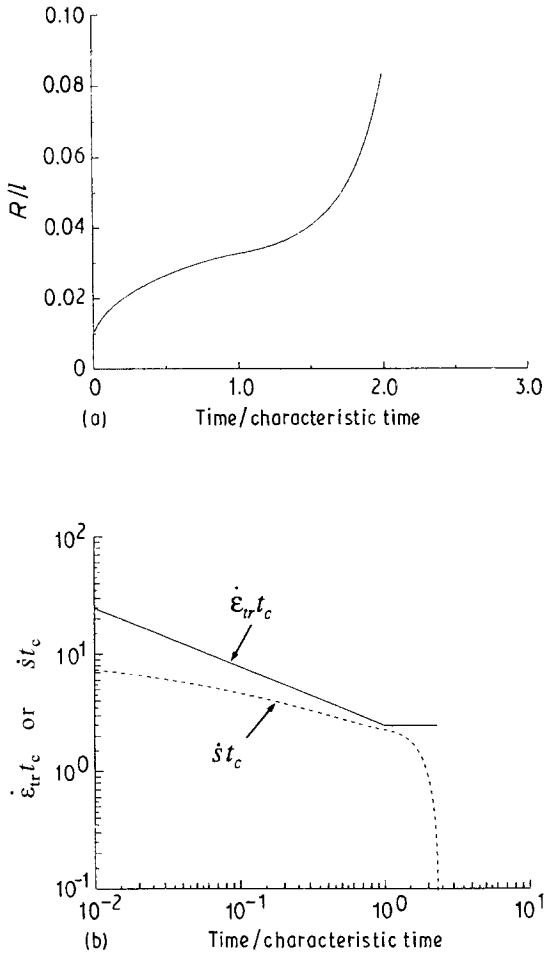

Figure 5 Calculated cavity radius, R, transient creep rate, $\dot{\varepsilon}_{tr}$, and sintering rate, $\dot{s}$, as functions of time normalized by the characteristic time, t_c, to attain the steady-state condition for $\dot{\varepsilon}_{ss}t_c = 2.46$: (a) cavity radius normalized by cavity spacing, R/l; $\xi_0 = 0.01$; $t_0 = 0.01$; $\gamma_s t_c/\eta l = 0.194$; (b) $\dot{\varepsilon}_{tr}t_c$ and $\dot{s}t_c$.

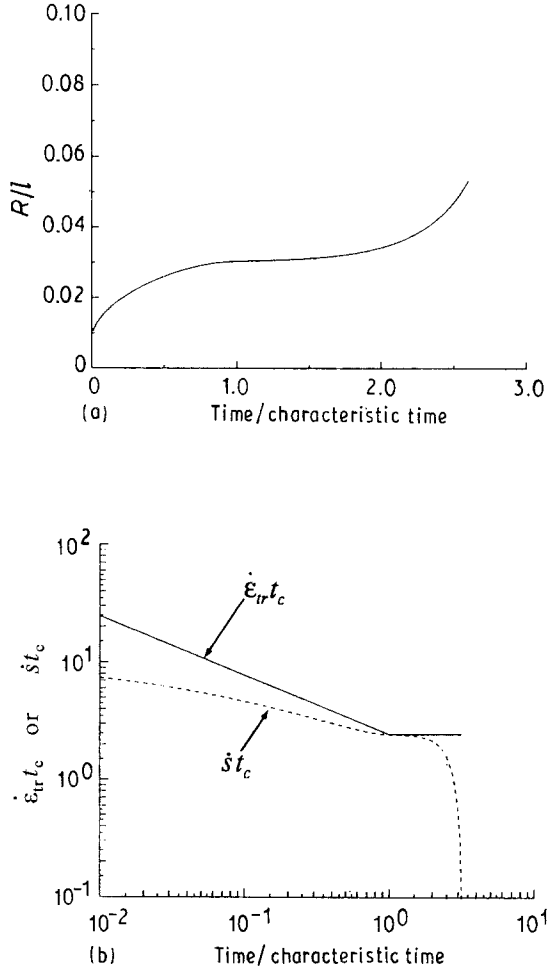

Figure 6 Calculated cavity radius, R, transient creep rate, $\dot{\varepsilon}_{tr}$, and sintering rate, $\dot{s}$, as functions of time normalized by the characteristic time, t_c, to attain the steady-state condition for $\dot{\varepsilon}_{ss}t_c = 2.455$: (a) cavity radius normalized by cavity spacing, R/l; $\xi_0 = 0.01$; $t_0 = 0.01$; $\gamma_s t_c/\eta l = 0.194$. (b) $\dot{\varepsilon}_{tr}t_c$ and $\dot{s}t_c$. Lowering of $\dot{\varepsilon}_{ss}t_c$ leads to a region of apparent zero cavity growth.

factor of three to five lower than that which can be achieved at a grain boundary containing a small (e.g. 10 μm) ledge. Based on the prescribed values, the cavity-growth behaviour was examined as a function of $\dot{\varepsilon}_{ss}t_c$ by integrating Equation 12, using a time increment of $0.0005t_c$.

Fig. 5a shows the cavity radius normalized by the cavity spacing, R/l, as a function of time normalized by the characteristic time, t/t_c, for the case of $\dot{\varepsilon}_{ss}t_c = 2.46$. Transient growth is evident in the regime where the normalized time is less than unity. The corresponding values of $\dot{\varepsilon}_{tr}$ and $\dot{s}$ are shown in Fig. 5b, which shows that $\dot{\varepsilon}_{tr}t_c$ decreases with increasing time and reaches the steady-state value when $t = t_c$. In addition, $\dot{\varepsilon}_{tr}$ is always greater than the sintering rate, $\dot{s}$. Consequently the cavity size increases at all times. When $\dot{\varepsilon}_{ss}t_c$ is lowered to 2.455, as shown in Fig. 6, a growth transient is observed initially, followed by an apparent zero growth region and subsequently by a rapid growth region. The corresponding results for $\dot{\varepsilon}_{tr}$ and $\dot{s}$ shown in Fig. 6b demonstrate that zero cavity growth occurs in the region where $\dot{\varepsilon}_{ss}$ approximately equals $\dot{s}$. Subsequent growth after the apparent zero-growth region is an indication that $\dot{\varepsilon}_{ss}$ is slightly larger than $\dot{s}$, rather than being identically equal. A true no-growth region is obtained when $\dot{\varepsilon}_{ss}t_c = 2.45432$ (Fig. 7) for which $\dot{\varepsilon}_{ss}$ equals $\dot{s}$ when $t > t_c$. When $\dot{\varepsilon}_{ss}$ is lowered still further to a value slightly less than $\dot{s}$, sintering occurs after an initial transient growth period; this behaviour is illustrated in Fig. 8.

The results in Figs 5–8 demonstrate that the prescribed value of the steady-state creep rate, $\dot{\varepsilon}_{ss}$, plays a significant role in the cavity growth kinetics even in the transient growth regime. This occurs because $\dot{\varepsilon}_{ss}$ scales $\dot{\varepsilon}_{tr}$, and thus represents the minimum creep rate that $\dot{s}$ must exceed in order to bring about cavity shrinkage. The influence of $\dot{\varepsilon}_{ss}$ on the cavity growth behaviour is summarized in Fig. 9 which illustrates the presence of a critical value of $\dot{\varepsilon}_{ss}$, $\dot{\varepsilon}_{cr}$, that leads to a no-growth behaviour. The value of $\dot{\varepsilon}_{cr}$ is influenced by the viscosity and surface energy, and they are related by the expression

$$\frac{\eta l \dot{\varepsilon}_{cr}}{\gamma_s} = \frac{4\pi}{33}(1/\xi - 0.9\xi) \qquad (15)$$

which is obtained from Equation 12 by setting $\dot{\xi} = 0$. As illustrated in Fig. 10, cavities exhibit continuous growth when $\dot{\varepsilon}_{ss}$ exceeds this critical value, but shrink when the opposite is true. The calculated normalized cavity size is presented against normalized time in Fig. 11. This shows that the time to achieve a certain value of R/l increases with decreasing values of $\dot{\varepsilon}_{ss}t_c$. If

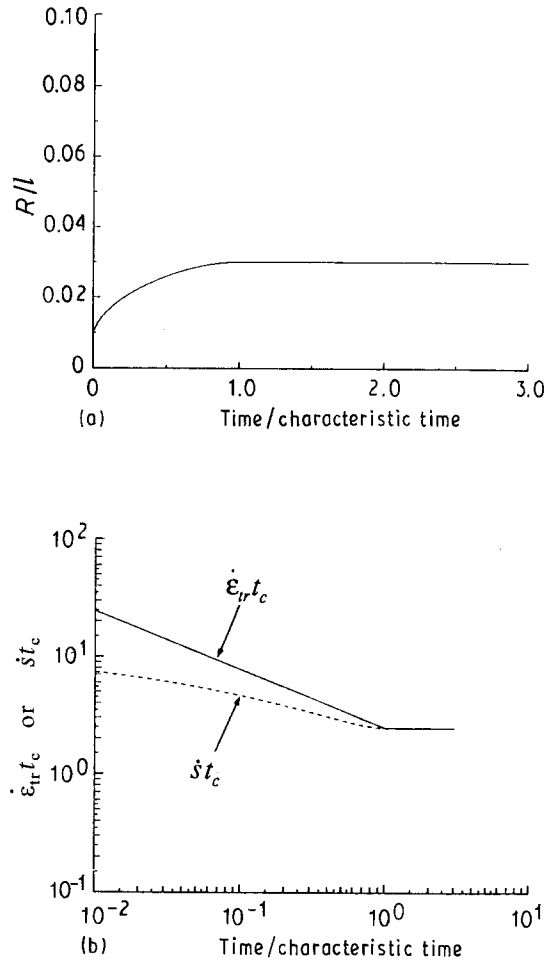

Figure 7 Calculated cavity radius, R, transient creep rate, $\dot{\varepsilon}_{tr}$, and sintering rate, $\dot{s}$, as functions of time normalized by the characteristic time, t_c, to attain the steady-state condition for $\dot{\varepsilon}_{ss}t_c = 2.45432$: (a) cavity radius normalized by cavity spacing, R/l; $\xi_0 = 0.01$; $t_0 = 0.01$; $\gamma_s t_c/\eta l = 0.01$. (b) $\dot{\varepsilon}_{tr}t_c$ and $\dot{s}t_c$. The balance between $\dot{\varepsilon}_{ss}$ and $\dot{s}$ leads to a true zero cavity growth region.

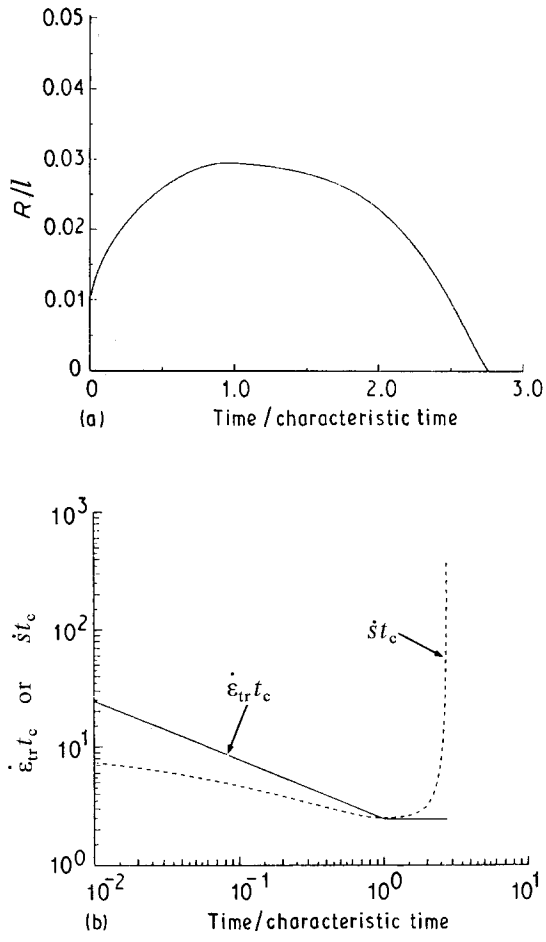

Figure 8 Calculated cavity radius, R, transient creep rate, $\dot{\varepsilon}_{tr}$, and sintering rate, $\dot{s}$, as functions of time normalized by the characteristic time, t_c, to attain the steady-state condition for $\dot{\varepsilon}_{ss}t_c = 2.453$: (a) cavity radius normalized by cavity spacing, R/l $\xi_0 = 0.01$; $t_0 = 0.01$; $\gamma_s t_c/\eta l = 0.194$. (b) $\dot{\varepsilon}_{tr}t_c$ and $\dot{s}t_c$. Reducing $\dot{\varepsilon}_{tr}$ to a value less than $\dot{s}$ leads to cavity shrinkage.

a specific value of R/l is taken as a failure criterion, the time to failure would increase with decreasing values of $\dot{\varepsilon}_{ss}t_c$ in a similar manner.

5. Comparison of model and experiment

The volumetric growth rate, $\dot{V}_{tr}$, of spheroidal cavities in the transient regime is

$$\dot{V}_{tr} = 4\pi R^2 \dot{R}$$

which becomes

$$\dot{V}_{tr} = \frac{33R^3G(\xi)}{\pi}(\dot{\varepsilon}_{tr} - \dot{s}) \qquad (16)$$

when combined with Equations 9, 11 and 14. A special case of Equation 16 is

$$\dot{V}_{tr} = \frac{33R^3G(\xi)}{\pi}\dot{\varepsilon}_{ss}(t/t_c)^m \qquad (17)$$

which prevails when $\dot{s}$ is negligible. Since the steady-state volumetric growth rate, V_{ss}, is given by [7]

$$\dot{V}_{ss} = \frac{33R^3G(\xi)\dot{\varepsilon}_{ss}}{\pi} \qquad (18)$$

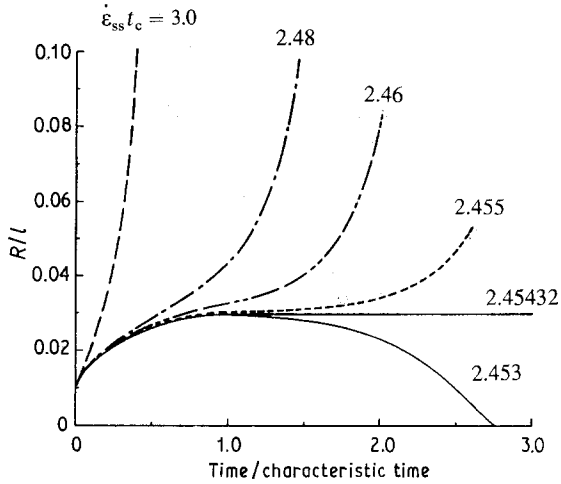

Figure 9 Influence of the steady-state creep rate, $\dot{\varepsilon}_{ss}$, on the cavity growth kinetics. The value of $\dot{\varepsilon}_{ss}$ must exceed a critical value, $\dot{\varepsilon}_{cr}$ (= 2.45432), in order to attain continuous cavity growth. $\xi_0 = 0.01$; $t_0 = 0.01$; $\gamma_s t_c/\eta l = 0.194$.

Equation 17 can be simplified to

$$\dot{V}_{tr} = \dot{V}_{ss}(t/t_c)^m \qquad (19)$$

for representing the volumetric growth rate of creep cavities subject to transient grain-boundary sliding.

TABLE II Summary of steady-state creep rate ($\dot{\varepsilon}_{ss}$), cavity volumetric growth rate ($\dot{V}$), and cavity nucleation rate ($\dot{n}$) as a function of time of creep, t, observed in ceramics

Material	T(°C)	Compressive stress(MPa)	$\dot{\varepsilon}_{ss}(s^{-1})$	$\dot{V}(cm^3 s^{-1})$	$\dot{n}$(Nuclei $cm^{-3} s$)
AD99[5]	1150	220	1.25×10^{-8}	$1.60 \times 10^{-17} t^{-0.77}$	$5.90 \times 10^{10} t^{-0.81}$
AD99[5]	1300	48	1.12×10^{-7}	$1.82 \times 10^{-16} t^{-0.70}$	$6.0 \times 10^{9} t^{-0.77}$
AD99[5]	1300	26	4.16×10^{-8}	0	$4.48 \times 10^{9} t^{-0.68}$
NC203[3]	1600	570	1.40×10^{-7}	$2.25 \times 10^{-19} t^{-0.37}$	0
NC203[3]	1600	605	2.80×10^{-7}	$5.66 \times 10^{-19} t^{-0.38}$	0
Lucalox[2]	1600	140	2.10×10^{-6}	0	3.13×10^{6}
Lucalox[2]	1600	140	8.10×10^{-7}	0	3.13×10^{6}

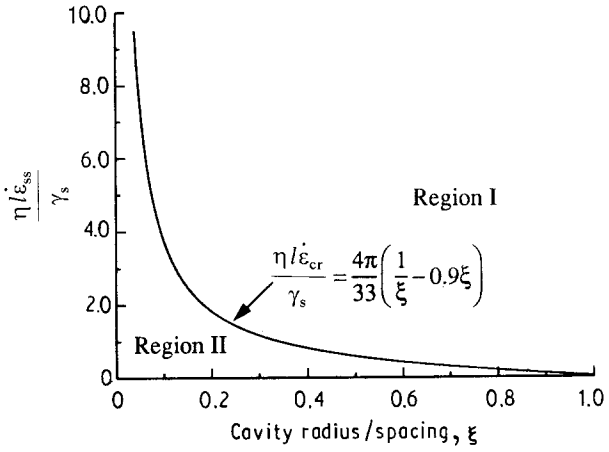

Figure 10 Regions of I, cavity growth and II, cavity shrinkage based on the proposed model. (—), zero cavity growth.

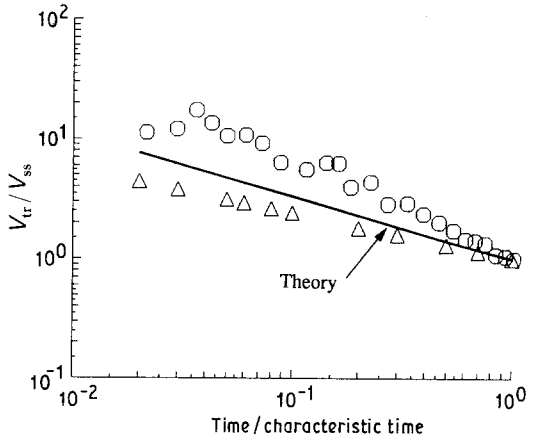

Figure 12 Comparison of the theoretical and experimental volumetric cavity growth rates. SANS measurement [3,5] ○, AD99; △, NC203.

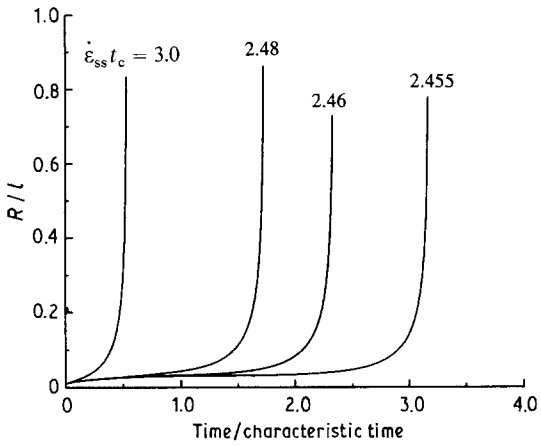

Figure 11 Model calculations showing the time to reach a constant ratio of cavity radius to spacing, R/l, increases with decreasing values of $\dot{\varepsilon}_{ss} t_c$. $\xi_0 = 0.01$; $t_0 = 0.01$; $\gamma_s t_c/\eta l = 0.194$.

A detailed examination of Equation 17 reveals that the transient cavity growth rate should increase linearly with the steady-state creep rate, primarily through Equation 9. A summary of the experimental creep rate and cavity volumetric growth rate for ceramics studied by Page and co-workers [2, 3, 5] is presented in Table II. For AD99 alumina crept at 1150 and 1300°C, a tenfold increase in $\dot{V}_{tr}$ was observed when the steady-state creep rate was increased by approximately the same magnitude. Similarly, a twofold increase in $\dot{V}_{tr}$ was observed in NC203 at 1600 °C when $\dot{\varepsilon}_{ss}$ was increased by a factor of two.

Another important observation from the results in Table II is that the cavity volumetric growth rate $\dot{V}$ expressions are similar in form for ceramics both with (AD99) and without (NC203) a grain-boundary amorphous phase. This similarity in the $\dot{V}$ expression appears to support the contention that Equations 9 and 19 can be used for describing, respectively, grain boundary sliding and cavity growth in ceramics with or without a glassy phase, providing that the appropriate characteristic time, t_c, is used.

A comparison of Equation 17 with experimental data from AD99 alumina and NC203 silicon carbide is shown in Fig. 12. The slope of the theoretical curve is -0.57, compared with the experimental values of -0.38 and -0.77 for NC203 silicon carbide and AD99 alumina, respectively. Despite the discrepancy, the qualitative agreement implies that the cavity growth transients observed in these ceramics originate directly from transient grain-boundary sliding. It is also instructive to note that Equation 19 is also applicable for the normal stress transient located at the ligament between two cavities. This condition has been analysed by Raj [8] using the Fourier series approach. His results showed a similar time dependence to that shown in Fig. 12 and represented by Equation 19. The normal stress transient is, however, thought not to be the mechanism responsible for transient growth in these ceramics because its characteristic time is much too short, as indicated above.

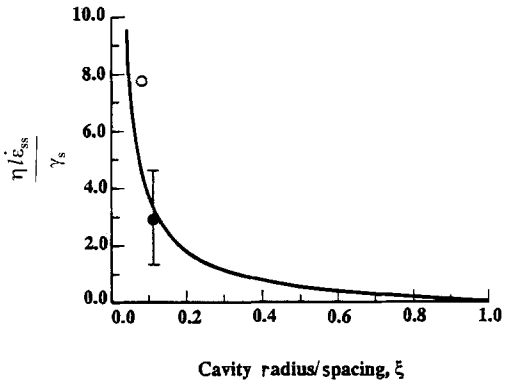

Figure 13 Comparison of the predicted (—) and experimentally observed conditions for zero cavity growth: ●, AD99, 1300 °C; ○, Lucalox, 1600 °C.

The zero-growth behaviour observed in these two ceramics can also be explained on the basis of transient grain-boundary sliding when Equation 15 is invoked to account for sintering effects. A quantitative comparison between model and experiment is shown in Fig. 13. The viscosity parameter, η, has been computed on the basis of Equation 4, and diffusion data compiled by Frost and Ashby [17]. For AD99 at 1300 °C, $hD_b \approx 1 \times 10^{-20}\ m^3\ sec^{-1}$, $d = 20$–$37\ \mu m$, $R = 8.0$ nm, and $l \approx 700$ nm. For Lucalox at 1600 °C, $hD_b \approx 2.7 \times 10^{-21}\ m^3\ s^{-1}$, $d = 37\ \mu m$, $R = 62$ nm, and $l \approx 700$ nm. The surface energy, γ_s, is taken to be $1\ J\ m^{-2}$, and the values for $\dot{\varepsilon}_{ss}$ are given in Table II. The viscosity parameter depends on the grain size; as a result, a range of values for $\eta\dot{\varepsilon}_{ss}l/\gamma_s$ is given for AD99 in Fig. 13. The comparison in this figure indicates fair agreement between theory and experiment.

At first glance, the zero cavity growth condition achieved through dynamic equilibrium of Equation 12 appeared to be rather difficult to obtain because a slight increase in the strain rate would lead to cavity growth, while a slight decrease would cause cavity sintering. However, a more detailed examination of the cavity growth process under constrained conditions suggested otherwise. In constrained cavitation, the local total strain rate, $\dot{\varepsilon}_t$, is given by

$$\dot{\varepsilon}_t = \dot{\varepsilon}_{gbs} + \dot{\varepsilon}_c + \dot{\varepsilon}_n + \dot{\varepsilon}_g \qquad (20)$$

where $\dot{\varepsilon}_{gbs} + \dot{\varepsilon}_c + \dot{\varepsilon}_n + \dot{\varepsilon}_g$ are strain rates contributed by grain-boundary sliding, creep, cavity nucleation and growth, respectively. The initial values for $\dot{\varepsilon}_n$ and $\dot{\varepsilon}_g$ were both zero prior to cavity nucleation and growth, but were of finite values after cavitation. Since the total strain rate for the cavitated region was controlled by the uncavitated surrounding matrix grains, any contribution to the local strain rate by cavity nucleation and growth in the cavitated region would lead to reductions in the amount of grain-boundary sliding and/or creep. A reduction in the grain-boundary sliding rate would slow or even arrest the growth of the cavities. The latter occurs when the cavity growth term intersected the sintering curve in a manner as shown in Fig. 7b. These cavities would not be sintered, however, because of continual grain-boundary sliding. A negative contribution by $\dot{\varepsilon}_n$ or $\dot{\varepsilon}_g$ due to sintering would lead to an increase in $\dot{\varepsilon}_{gbs}$; this would lead to cavity growth and restore the cavities to their no-growth configuration. Under these circumstances, cavitation would occur by continuous nucleation of cavities which would not grow beyond a given size. This process would proceed until cavities are nucleated at neighbouring boundaries, and cavitation would then proceed in an unconstrained manner. This proposed cavitation process is consistent with the results shown in Table II, which indicates that cavity nucleation is the dominant mechanism when zero cavity growth is observed.

6. Conclusions

1. The transient cavity growth observed in ceramics under compressive loading is probably induced by transient grain-boundary sliding.

2. Zero cavity growth prevails in ceramics under compression when the local tensile stress induced by grain-boundary sliding is balanced by the sintering term. The condition of zero cavity growth occurs at a critical value of the steady-state creep rate.

3. There exists a critical value, $\dot{\varepsilon}_{cr}$, of the steady-state creep rate which must be exceeded in order for continuous cavity growth to occur. The value of $\dot{\varepsilon}_{cr}$ depends on grain-boundary viscosity, surface energy, cavity size and spacing.

Acknowledgements

The support of this work by the US Department of Energy, Office of Basic Energy Science, through Grant No. DE-FGO5-84ER45063 is gratefully acknowledged.

References

1. R. A. PAGE and J. LANKFORD, *J. Amer. Ceram. Soc.* **66** (1983) C-146.
2. R. A. PAGE, J. LANKFORD and S. SPOONER, *J. Mater. Sci.* **19** (1984) 3360.
3. *Idem, Acta Metall.* **32** (1984) 1275.
4. J. LANKFORD, K. S. CHAN and R. A. PAGE, in "Fracture Mechanics of Ceramics," edited by R. C. Bradt, A. G. Evans, D. P. H. Hasselman and F. F. Lange (Plenum, New York, 1986) p. 327.
5. R. A. PAGE, J. LANKFORD, K. S. CHAN, K. HARDMAN-RHYNE and S. SPOONER, *J. Amer. Ceram. Soc.* **70** (1987) 137.
6. K. S. CHAN and R. A. PAGE, *Metall. Trans. A* **18A** (1987) 1843.
7. K. S. CHAN, J. LANKFORD and R. A. PAGE, *Acta Metall.* **32** (1984) 1908.
8. R. RAJ, *Metall. Trans. A* **6A** (1975) 1499.
9. K. S. CHAN and R. A. PAGE, *J. Mater. Sci.* **25** (1990) 4622.
10. B. L. VAANDRAGER and G. M. PHARR, *Acta Metall.* **37** (1989) 1057.
11. J. R. DRYDEN, D. KUCEROVSKY, D. S. WILKINSON and D. F. WATT, *Acta Metall.* **37** (1989) 2007.
12. R. RAJ and M. F. ASHBY, *Metall. Trans. A* **2** (1971) 1113.
13. R. RAJ and C. K. CHYUNG, *Acta Metall.* **29** (1981) 159.
14. S. M. WIEDERHORN, B. J. HOCKEY, R. F. KRAUSE, Jr. and K. JAKUS, *J. Mater. Sci.* **21** (1986) 810.
15. E. H. RUTTER, *Trans. Roy. Soc. A* **283** (1976) 203.
16. K. S. CHAN, R. A. PAGE and J. LANKFORD, *Acta Metall.* **34** (1986) 2361.
17. H. J. FROST and M. F. ASHBY, "Deformation-Mechanism Maps" (Pergamon, New York, 1982) p. 98.

Received 21 November 1990
and accepted 10 April 1991